Molecular Crystals and Liquid Crystals
Publication details, including instructions for authors and subscription information:
http://www.tandfonline.com/loi/gmcl20

Thermodynamic Studies on Solid Dispersions of Nicotinamide - Khellin Drug System

H. Shekhar [a] & Vishnu Kant [a]
[a] Department of Chemistry , V. K. S. University , Ara , Bihar , India
Published online: 09 Jul 2013.

To cite this article: H. Shekhar & Vishnu Kant (2013) Thermodynamic Studies on Solid Dispersions of Nicotinamide - Khellin Drug System, Molecular Crystals and Liquid Crystals, 577:1, 103-115, DOI: 10.1080/15421406.2013.782207

To link to this article: http://dx.doi.org/10.1080/15421406.2013.782207

Mol. Cryst. Liq. Cryst., Vol. 577: pp. 103–115, 2013

ISSN: 1542-1406 print/1563-5287 online
DOI: 10.1080/15421406.2013.782207

Taylor & Francis
Taylor & Francis Group

Thermodynamic Studies on Solid Dispersions of Nicotinamide – Khellin Drug System

H. SHEKHAR* AND VISHNU KANT

Department of Chemistry, V. K. S. University, Ara, Bihar, India

Biomolecules, nicotinamide (NA), and khellin (KH) have been used orally for a number of diseases for the last few decades. NA is shown as an HIV, Mycobaterium tuberculosis, and pellagra preventive agent, whereas KH is used in renal colic, diuretic, kidney stone, coronary, bronchial asthma, angina, vitiligo, and psoriasis. In recent years, research on solid dispersions of binary drug products is playing a significant role in the drug delivery process of the pharmaceutical industries. The present study highlights the thermodynamic characteristics of solid dispersions binary products of active pharmaceutical ingredient KH with pharmaceutical excipient NA. These products have been prepared through melting/fusion method. The solid–liquid equilibrium (SLE) data of NA–KH system favors the formation of an eutectic (E) at 0.135 mole fraction of KH and melting temperature 120.6°C and noneutectic solid dispersions (A1–A8) at their defined compositions and temperatures. To illustrate the molecular interaction, the activity coefficient model based on enthalpy of fusion is employed to calculate the excess partial and integral thermodynamic functions such as g^E, h^E, and s^E. The positive value of excess Gibbs free energy predicts the stronger molecular interaction between the like molecules as compared to unlike molecules. The spontaneity of mixing of eutectic and noneutectic alloys was discussed by the integral mixing quantities ΔG^M, ΔH^M , and ΔS^M. The value of critical radius (r^*) of solid dispersions is found in nanometer (nm) scale, which suggests the process of solidification for nanosolid dispersions, and it is very surprising for the pharma world. The binary interface structure of alloys has been discussed in light of the Jackson model of interface structure.

Keywords Critical radius; interfacial energy; roughness parameter; solid–liquid equilibrium data; thermodynamic excess and mixing functions

Introduction

Heterocycles are important biological and pharmacological active chemical entities. The research and development on this class of compounds have provided myriad applications in medicines and food production over past few decades. Nicotinamide (NA) is a structural component of nicotinamide adenine dinucleotide (NAD) and nicotinamide adenine dinucleotide phosphate (NADP), which have very important coenzymic role in metabolic oxidation–reduction reactions in human being. It is water soluble vitamin B_3 and a part of vitamin B-complex. It is anti-HIV [1], anti-*M. tuberculosis* [2], anti-inflammatory [3], and antipellagra [4] agent. Khellin (KH) [5] has been used for the treatment of urologic, dermatologic, and respiratory symptoms. It is effective in the relaxation of the gall bladder, bile duct, and urinary bladder. It has been demonstrated to be a much safer drug [6] than

*Address correspondence to H. Shekhar, Department of Chemistry, V. K. S. University, Ara 802301, India. E-mail: hshe2503@reiffmail.com

psoralen derivatives, because it is much less genotoxic and phototoxic. Much of the interest in KH was directed at its action on the heart, following a serendipitous observation [7] that it is renal colic and angina remover. It is also used as a spasmolitic agent in the therapy of asthma and angina pectoris, and recently its use has been proposed for the treatment of vitiligo [8] and psoriasis. Eutectic and noneutectic solid dispersions [9,10] of active pharmaceutical hydrophobic ingredients with hydrophilic excipient NA are important due to their ability to control pharmaceutical properties without changing covalent bonds of the parent components as well as they can be used in designing [11] of new materials. In recent years, advances in supramolecular engineering and chemistry have motivated to extend research on the design of pharmaceutical materials by directing molecular association of different components in the crystalline state to form binary/ternary solid dispersions of potential interest. Pharmaceutical properties of some binary solid dispersions have also been reported [12,13] with account of their enhanced solubility, dissolution rate, hygroscopicity, and chemical stability. Eutectic mixture formation between NA and hydrophobic carriers/drugs of different therapeutic classes was investigated [14,15] recently to reduce the drug particle size and increases the dissolution rate and thus changes the biopharmaceutical properties. Keeping in view the pharmacological importance, NA–KH drug system was selected for the solid–liquid equilibrium (SLE), thermodynamic and interfacial investigations of eutectic and noneutectic solid dispersions drugs.

Experimental Details

Nicotinamide (Thomos Baker, India) and KH were directly taken for investigation. The melting point of NA was found to be 128°C while for KH it was found to be 153°C. For measuring the SLE data of NA–KH system, mixtures of different compositions of both were made in glass test tubes by repeated heating and followed by chilling in ice, and melting temperatures of solid dispersions were determined by the thaw-melt method [16]. The melting and thaw temperatures were determined in a Toshniwal melting point apparatus using a precision thermometer, which could read correctly up to ±0.1°C. The heater was regulated to give above 1°C increase in temperature in every 5 minutes. The literature value [17] of enthalpy of fusion of NA and KH was used in determining the various thermodynamic parameters of the binary system.

Result and Discussion

SLE Study

The SLE data of NA–KH system determined by the thaw-melt method is reported in Table 1. The system shows the formation of an eutectic (E) [18] and noneutectics solid dispersions (A1–A8). The melting point of NA (128°C) decreases on the addition of second component KH (mp, 153°C) and further attains minimum and then increases. Eutectic E (0.135 mole fraction of KH) is obtained at 120.6°C. At the eutectic temperature, a liquid phase L and two solid phases (S_1 and S_2) are in equilibrium and the system is invariant. The homogenous binary liquid solution exists in the region above the eutectic temperature, whereas the two solid phases exist in the region below the eutectic temperature. The region located below the liquidus line on the left side, a binary liquid and solid NA exist, whereas in a similar region located on the right side, a binary liquid and solid KH system coexist.

$$L \overset{\text{cooling}}{\rightleftharpoons} S_1 + S_2$$

Table 1. Phase composition, melting temperature, values of entropy of fusion per unit volume (ΔS_v), heat of fusion (ΔH), interfacial energy (σ), grain boundary energy (σ_{gb}), Gibbs–Thomson coefficient (τ), and roughness parameter (α)

Alloy	χ_{NA}	χ_{KH}	MP	ΔH ($J \cdot mol^{-1}$)	ΔS ($J \cdot mol^{-1} \cdot K^{-1}$)	α	$\sigma \times 10^2$ ($J \cdot m^{-2}$)	$\sigma_{gb} \times 10^2$ ($J \cdot m^{-2}$)	ΔS_v ($kJ \cdot m^{-3} \cdot K^{-1}$)	ΔH_v	$\tau \times 10^5$ km
A1	0.035	0.965	151.0	32058.5	75.61	9.09	3.712	7.17	386	163.495	1.859
A2	0.110	0.890	149.5	31541	74.653	8.98	3.761	7.265	398	168.108	1.826
A3	0.305	0.695	141.5	30195.5	72.848	8.76	3.912	7.558	440	182.309	1.710
A4	0.440	0.560	134.8	29264	71.761	8.63	4.043	7.811	477	194.573	1.637
A5	0.600	0.400	132.5	28160	69.445	8.35	4.237	8.185	525	212.763	1.560
A6	0.700	0.300	130.5	27470	68.079	8.19	4.386	8.473	562	226.886	1.507
E	0.865	0.135	120.6	26331.5	66.899	8.05	4.699	9.078	653	256.985	1.390
A7	0.900	0.100	123.0	26090	65.884	7.92	4.779	9.233	669	264.832	1.381
A8	0.953	0.047	125.5	25724.3	64.553	7.76	4.913	9.492	698	277.989	1.361
NA			128	25400	63.342	7.62	5.046	9.748	726	291.165	1.343
KH			153	32300	75.822	9.12	3.69	7.129	379	161.475	1.881

Thermodynamic Study

The values of heats of fusion of eutectic and noneutectic are calculated by the mixture law. The value of heat of fusion of binary solid dispersions A_1–A_8 and E is reported in Table 1. The activity coefficient and activity of components for the systems under investigation has been calculated from the equation [19] given below

$$-\ln\chi_i\gamma_i = \frac{\Delta H_i}{R}\left(\frac{1}{T_e} - \frac{1}{T_i}\right) \tag{1}$$

where χ_i, γ_i are the mole fraction and activity coefficient of the component i in the liquid phase, respectively. ΔHi is the heat of fusion of component i at its melting point T_i, and R is the gas constant. T_e is the melting temperature of alloy. Using the values of activity and activity coefficient of the components in the binary product, the mixing and excess thermodynamic functions have been evaluated.

Mixing Functions

To know the mixing characteristics of components in the system, integral molar free energy of mixing (ΔG^{M}), molar entropy of mixing (ΔS^{M}), molar enthalpy of mixing (ΔH^{M}), and partial thermodynamic mixing functions of the binary solid dispersions were determined by using the following equations

$$\Delta G^{\mathrm{M}} = RT\ (\chi_{\mathrm{NA}}\ \ln a_{\mathrm{NA}} + \chi_{\mathrm{KH}}\ \ln a_{\mathrm{KH}}) \tag{2}$$

$$\Delta S^{\mathrm{M}} = -R\ (\chi_{\mathrm{NA}}\ \ln\chi_{\mathrm{NA}} + \chi_{\mathrm{KH}}\ \ln\chi_{\mathrm{KH}}) \tag{3}$$

$$\Delta H^{\mathrm{M}} = RT\ (\chi_{\mathrm{NA}}\ \ln\gamma_{\mathrm{NA}} + \chi_{\mathrm{KH}}\ \ln\gamma_{\mathrm{KH}}) \tag{4}$$

$$G_i^- M = \mu_i^- M = RT\ln a_i. \tag{5}$$

where $G^-{}_i^{\mathrm{M}}$ ($\mu^-{}_i^{\mathrm{M}}$) is the partial molar free energy of mixing of component i (mixing chemical potential) in binary mix and γi and ai are the activity coefficient and activity of component, respectively. The positive value [20] of molar free energy of mixing of alloys (Table 2) suggests that the mixing in all cases is nonspontaneous. The integral molar enthalpy of mixing value corresponds to the value of excess integral molar free energy of the system favors the regularity in the binary solutions.

Excess Functions

To unfold the nature of the interactions between the components forming the eutectic and noneutectic solid dispersions, the excess thermodynamic functions such as integral excess integral free energy (g^{E}), excess integral entropy (s^{E}), and excess integral enthalpy (h^{E}) were calculated using the following equations

$$g^{\mathrm{E}} = RT(\chi_{\mathrm{NA}}\ln\gamma_{\mathrm{NA}} + \chi_{\mathrm{KH}}\ln\gamma_{\mathrm{KH}}) \tag{6}$$

$$s^E = -R\left((\chi_{\mathrm{NA}}\ln\gamma_{\mathrm{NA}} + \chi_{\mathrm{KH}}\ln\gamma_{\mathrm{KH}} + \chi_{\mathrm{NA}}T\frac{\delta\ln\gamma_{\mathrm{NA}}}{\delta T} + \chi_{\mathrm{KH}}T\frac{\delta\ln\gamma_{\mathrm{KH}}}{\delta T}\right) \tag{7}$$

$$h^E = -RT^2\left(\chi_{\mathrm{NA}}\frac{\delta\ln\gamma_{\mathrm{NA}}}{\delta T} + \chi_{\mathrm{KH}}\frac{\delta\ln\gamma_{\mathrm{KH}}}{\delta T}\right) \tag{8}$$

Table 2. Value of partial and integral mixing of Gibbs free energy (ΔG^{M}), enthalpy (ΔH^{M}), and entropy (ΔS^{M}) of NA–KH system

Alloy	$\Delta G_{NA}{}^{-M}$ ($J \cdot mol^{-1}$)	$\Delta G_{KH}{}^{-M}$ ($J \cdot mol^{-1}$)	ΔG^{M} ($J \cdot mol^{-1}$)	$\Delta H_{NA}{}^{-M}$ ($J \cdot mol^{-1}$)	$\Delta H_{KH}{}^{-M}$ ($J \cdot mol^{-1}$)	ΔH^{M} ($J \cdot mol^{-1}$)	$\Delta S_{NA}{}^{-M}$ ($J \cdot mol^{-1} \cdot K^{-1}$)	$\Delta S_{KH}{}^{-M}$ ($J \cdot mol^{-1} \cdot K^{-1}$)	ΔS^{M} ($J \cdot mol^{-1} \cdot K^{-1}$)
A1	25092.24	99.5381	974.2827	13274.55	−26.053	−439.469	27.872	0.296	1.261
A2	16868.68	553.3129	2348.003	9115.263	143.969	−1130.81	18.351	0.969	2.881
A3	9039.336	1635.772	3893.859	4947.224	381.912	−1774.33	9.8724	3.025	5.113
A4	5997.709	2551.737	4067.965	3214.216	585.892	−1742.35	6.8256	4.821	5.703
A5	3729.358	4623.889	4087.17	2007.198	1534.77	−1818.23	4.247	7.618	5.595
A6	2551.428	6371.947	3697.584	1354.891	2332.98	−1648.32	2.9654	10.01	5.079
E	480.4337	10649.18	1853.214	5.852765	4096.28	−558.06	1.2057	16.65	3.291
A7	377.0579	12887.16	1628.068	30.17483	5306.25	−557.783	0.876	19.14	2.703
A8	160.6364	18175.4	1007.33	1.141159	8045.15	−379.21	0.4002	25.42	1.576

and excess chemical potential or excess partial free energy of mixing

$$g_i^{-\mathrm{E}} = \mu_i^{-\mathrm{M}} = RT \ln \gamma_i. \tag{9}$$

The values of $\delta \ln \gamma_i / \delta T$ can be determined by the slope of liquidus curve near the alloys. The values of the excess thermodynamic functions are given in Table 3. The value of the excess free energy is a measure of the departure of the system from ideal behavior. The reported excess thermodynamic data substantiate the earlier conclusion of an appreciable interaction between the parent components during the formation of alloys. The positive g^{E} value [21] for all eutectic and noneutectic solid dispersions infers stronger interaction between like molecules in binary mix. The excess entropy is a measure of the change in configurational energy due to a change in potential energy and indicates an increase in randomness.

Gibbs–Duhem Equation

Furthermore, the partial molar quantity, activity, and activity coefficient can also be determined by using Gibbs–Duhem equation [22]

$$\sum \chi_i dz_i^{-\mathrm{M}} = 0 \tag{10}$$

or

$$\chi_{\mathrm{NA}} dH_{\mathrm{NA}}^{-\mathrm{M}} + \chi_{\mathrm{KH}} dH_{\mathrm{KH}}^{-\mathrm{M}} = 0 \tag{11}$$

or

$$dH_{\mathrm{NA}}^{-\mathrm{M}} = \frac{\chi_{\mathrm{KH}}}{\chi_{\mathrm{NA}}} dH_{\mathrm{KH}}^{-\mathrm{M}} \tag{12}$$

or

$$[H_{\mathrm{NA}}^{-\mathrm{M}}]_{x_{\mathrm{NA}}=y} = \int_{\chi_{\mathrm{NA}}=y}^{\chi_{NA}=1} \frac{\chi_{\mathrm{KH}}}{\chi_{\mathrm{NA}}} dH_{\mathrm{KH}}^{-\mathrm{M}}. \tag{13}$$

Using Equation (13), a graph (Fig. 1) between $H_{\mathrm{KH}}^{-\mathrm{M}}$and $\chi_{\mathrm{KH}}/\chi_{\mathrm{NA}}$ gives the solution of the partial molar heat of mixing of a constituent NA in binary mix, and plot between $\chi_{\mathrm{KH}}/\chi_{\mathrm{NA}}$ versus $\ln a_{\mathrm{KH}}$ determines the value of activity (Fig. 2) of component NA in binary mix.

Interfacial Investigation

The Solid–Liquid Interfacial Energy (σ)

It has been realized that an experimentally observed value of interfacial energy "σ" keeps a variation of 50%–100% from one worker to other. However, Singh and Glicksman [23] calculated the solid–liquid interfacial energy (σ) from melting enthalpy change, and values obtained are found in good agreement with the experimental values. Turnbull empirical relationship [24] between the interfacial energy and enthalpy change provides the clue to determine the interfacial energy value of binary solid dispersions and is expressed as

$$\sigma = \frac{C \Delta H}{(N)^{1/3} (V_{\mathrm{m}})^{2/3}} \tag{14}$$

Table 3. Value of partial and integral excess Gibbs free energy (g^E), enthalpy (h^E), and entropy (s^E) of NA–KH system

Alloy	$g_{NA}{}^{-E}$ ($J \cdot mol^{-1}$)	$g_{KH}{}^{-E}$ ($J \cdot mol^{-1}$)	g^E ($J \cdot mol^{-1}$)	$h_{NA}{}^{-E}$ ($J \cdot mol^{-1}$)	$h_{KH}{}^{-E}$ ($J \cdot mol^{-1}$)	h^E ($J \cdot mol^{-1}$) J/mol	$s_{NA}{}^{-E}$ ($J \cdot mol^{-1} \cdot K^{-1}$)	$s_{KH}{}^{-E}$ ($J \cdot mol^{-1} \cdot K^{-1}$)	s^E ($J \cdot mol^{-1} \cdot K^{-1}$)
A1	13274.55	−26.053	439.469	1127622	9519.437	48653	2628.18	22.513	113.71
A2	9115.263	143.969	1130.81	379354.8	17725.88	57505.1	876.307	41.614	133.43
A3	4947.224	381.912	1774.33	82317.7	14971.8	35512.3	186.66	35.199	81.394
A4	3214.216	585.892	1742.35	46873.59	24486.39	34336.8	107.061	58.608	79.927
A5	2007.198	1534.77	1818.23	122699.6	189849.4	149560	297.638	464.4	364.34
A6	1354.891	2332.98	1648.32	32612.33	103062.1	53747.3	77.4658	249.64	129.12
E	5.852765	4096.28	558.06	19270.97	253925.1	50949.3	48.9459	634.73	128.03
A7	30.17483	5306.25	557.783	−773.267	189340.6	18238.1	−2.0289	464.73	44.647
A8	1.141159	8045.15	379.21	2307.91	529522.1	27087	5.78863	1308.6	67.021

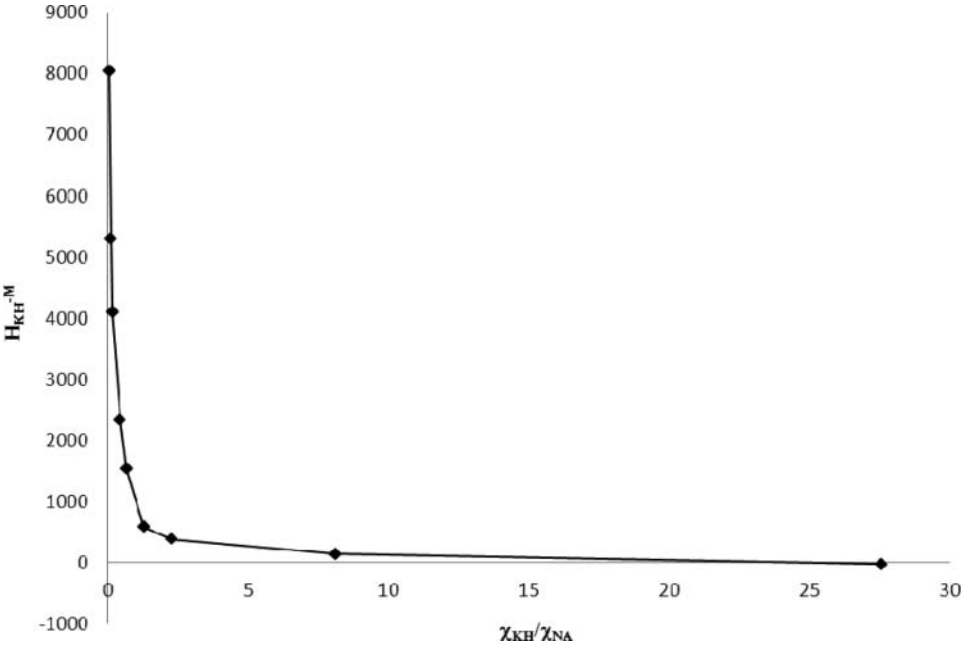

Figure 1. Graphical solution of partial molar enthalpy of mixing of KH in binary mix.

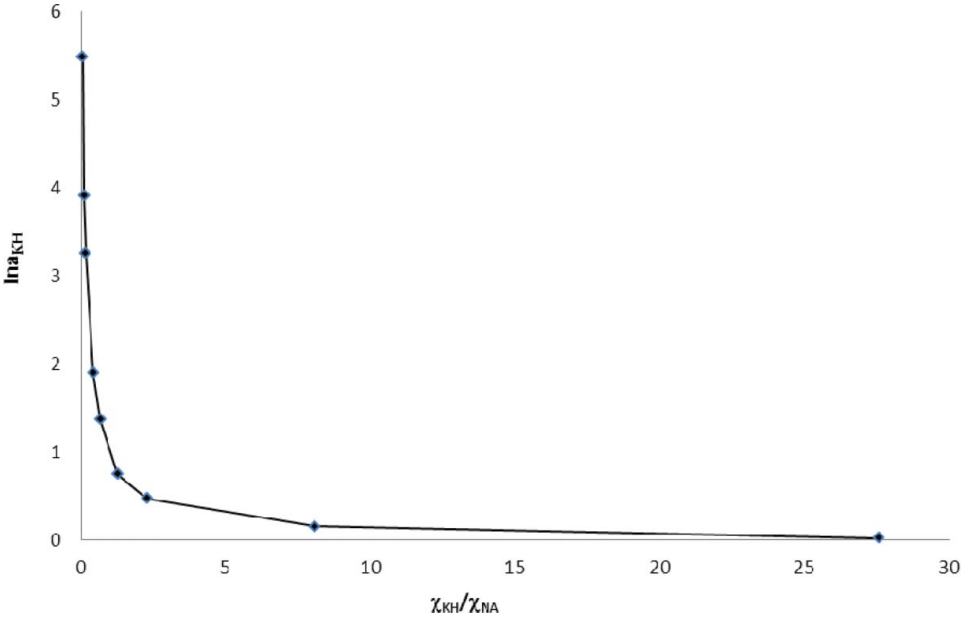

Figure 2. Graphical solution of activity of KH in binary mixture.

where the coefficient C lies between 0.33 to 0.35 for nonmetallic system, V_m is molar volume and N is the Avogadro's constant. The value of the solid–liquid interfacial energy of NA and KH was found to be 5.046×10^{-02} and 3.690×10^{-02} J · m^{-2}, respectively, and σ value of the solid dispersions was given in Table 1. The value of σ has also been determined by using the value of Gibbs–Thomson coefficient. The theoretical basis of determination of τ was made for equal thermal conductivities of solid and liquid phases for some transparent materials.

Gibbs–Thomson Coefficient (τ)

For a planar grain boundary on planar solid–liquid interface, the Gibbs–Thomson coefficient (τ) for the system can be calculated by the Gibbs–Thomson equation and is expressed as

$$\tau = r\Delta T = \frac{TV_m\sigma}{\Delta H} = \frac{\sigma}{\Delta S_V} \tag{15}$$

where τ is the Gibbs–Thomson coefficient, ΔT is the dispersion in equilibrium temperature, and r is the radius of grooves of interface. It was also determined by the help of Gunduz and Hunt [25] numerical method for materials having known grain boundary shape, temperature gradient in solid, and the ratio of thermal conductivity of the equilibrated liquid phases to solid phase ($R = K_L/K_S$). The Gibbs–Thomson coefficient for NA, KH, and their solid dispersions are found in the range of $1.321–1.480 \times 10^{-05}$ km and is reported in Table 1.

Interfacial Grain Boundary Energy (σ_{gb})

Grain boundary is the internal surface, which can be understood in a very similar way to nucleation on surfaces in liquid–solid transformation. In the past, a numerical method [26] is applied to observe the interfacial grain boundary energy (σ_{gb}) without applying the temperature gradient for the grain boundary groove shape. For isotropic interface, there is no difference in the value of interfacial tension and interfacial energy. A considerable force is employed at the grain boundary groove in anisotropic interface. The grain boundary energy can be obtained by the equation

$$\sigma_{gb} = 2\sigma \cos\theta \tag{16}$$

where θ is equilibrium contact angle precipitates at solid–liquid interface of grain boundary. The grain boundary energy could be twice the solid–liquid interfacial energy in the case where the contact angle tends to zero. The value of σ_{gb} for solid NA and KH was found to be 9.748×10^{-2} and 7.129×10^{-2} J · m^{-2}, respectively, and the value for all solid dispersions is given in Table 1.

The Effective Entropy Change (ΔS_v)

It is obvious that the effective entropy change and the volume fraction of phases in the alloy are interrelated to decide the interface morphology during solidification, and the volume fraction of the two phases depends on the ratio of effective entropy change of the phases. The entropy of fusion ($\Delta S = \Delta H/T$) value (Table 1) of alloys is calculated by heat of fusion values of the materials. The effective entropy change per unit volume (ΔS_V) is given by

$$\Delta S_V = \frac{\Delta H}{T}\frac{1}{V_m} \tag{17}$$

Table 4. Value of volume free energy change (ΔG_v) during solidification for NA–KH system of different undercoolings (ΔT)

	ΔG_v ($J \cdot cm^{-3}$)					
Alloy	1.0	1.5	2.0	2.5	3.0	3.5
A1	0.386	0.578	0.771	0.964	1.157	1.35
A2	0.398	0.597	0.796	0.995	1.194	1.393
A3	0.44	0.66	0.88	1.1	1.319	1.539
A4	0.477	0.716	0.954	1.193	1.431	1.67
A5	0.525	0.787	1.049	1.312	1.574	1.836
A6	0.562	0.843	1.125	1.406	1.687	1.968
E	0.653	0.979	1.306	1.632	1.959	2.285
A7	0.669	1.003	1.338	1.672	2.006	2.341
A8	0.698	1.046	1.395	1.744	2.093	2.442
NA	0.726	1.089	1.452	1.815	2.178	2.541
KH	0.379	0.569	0.758	0.948	1.137	1.327

where ΔH is the enthalpy change, T is the melting temperature, and V_m is the molar volume of solid phase. The entropy of fusion per unit volume (ΔS_V) for NA and KH was found to be 726 and 379 $kJ \cdot K^{-1} \cdot m^{-3}$, respectively. Values of ΔS_V for alloys are reported in Table 1.

The Driving Force of Nucleation (ΔG_v)

During growth of crystalline solid, there is change in enthalpy, entropy, and specific volume, and nonequilibrium leads the Gibbs energy. Thermodynamically metastable phase occurs in a supersaturated or supercooled liquid. The driving force for liquid–solid transition is the difference in Gibbs energy between the two phases. The theories of solidification process in the past have been discussed on the basis of diffusion model, kinetic characteristics of nucleation, and thermodynamic features. The lateral motion of rudimentary steps in liquid advances stepwise with nonuniform surface at low driving force, whereas continuous and uniform surface advances at sufficiently high driving force. The driving force of nucleation from liquid to solid during solidification (ΔG_V) can be determined at different undercoolings (ΔT) by using the following equation [27]

$$\Delta G_V = \Delta S_v \Delta T. \tag{18}$$

It is opposed by the increase in surface free energy due to creation of a new solid–liquid interface. By assuming that solid phase nucleates as small spherical cluster of radius arising due to random motion of atoms within liquid. The value of ΔG_V for each solid dispersions and pure components are shown in the Table 4.

The Critical Radius (r)*

During liquid–solid transformation, embryos are rapidly dispersed in unsaturated liquid, and on undercooling, liquid becomes saturated and provides embryo of a critical size with

Table 5. Critical size of nucleus (r^*) at different undercoolings (ΔT)

	r^* (nm)					
Alloy	1.0	1.5	2.0	2.5	3.0	3.5
A1	192.5	128.3	96.3	77.0	64.2	55.0
A2	189.0	126.0	94.5	75.6	63.0	54.0
A3	177.9	118.6	88.9	71.2	59.3	5.08
A4	169.5	113.0	84.7	67.8	56.5	48.4
A5	161.5	107.7	80.7	64.6	53.8	46.1
A6	156.0	104.0	78.0	62.4	52.0	44.6
E	143.9	96.0	72.0	57.6	48.0	41.1
A7	142.9	953	71.5	57.2	47.6	40.8
A8	140.9	93.9	70.4	56.3	47.0	40.2
NA	139.0	92.7	69.5	55.6	46.3	39.7
KH	194.7	129.8	97.3	77.9	64.9	55.6

radius r^* for nucleation, which can be determined by the Chadwick relation [28]

$$r^* = \frac{2\sigma}{\Delta G_V} = \frac{2\sigma T}{\Delta H_V \Delta T} \tag{19}$$

where σ is the interfacial energy and ΔH_V is the enthalpy of fusion of the compound per unit volume, respectively. The critical size of the nucleus for the components and alloys was calculated at different undercoolings, and values are presented in Table 5. It can be inferred from table that the size of the critical nucleus decreases with increase in the undercooling of the melt. The existence of embryo and a range of embryo size can be expected in the liquid at any temperature. The value of r^* for pure components (NA and KH) and solid dispersions lies between 39 to 195 nm at undercooling 1°C –3.5°C.

Critical Free Energy of Nucleation (ΔG^*)

To form critical nucleus, it requires a localized activation/critical free energy of nucleation (ΔG^*), which is evaluated [29] as

$$\Delta G^* = \frac{16}{3} \frac{\pi \sigma^3}{\Delta G_v^2}. \tag{20}$$

The value of ΔG^* for alloys and pure components has been found in the range of 10^{-15} to 10^{-16} J per molecule at different undercoolings and has been reported in Table 6.

Interface Morphology

The science of growth has been developed on the foundation of thermodynamics, kinetics, fluid dynamics, crystal structures, and interfacial sciences. The solid–liquid interface morphology can be predicted from the value of the entropy of fusion. According to Hunt and Jackson [30], the type of growth from a binary melt depends upon a factor α, which defined

Table 6. Value of critical free energy of nucleation (ΔG^*) for alloys of NA–KH system at different undercooling (ΔT)

	$\Delta G^* \times 10^{16}$ (J)					
Alloy	1.0	1.5	2.0	2.5	3.0	3.5
A1	57.64	25.62	14.41	9.22	6.40	4.70
A2	56.31	25.03	14.08	9.01	6.26	4.60
A3	51.89	23.06	12.97	8.30	5.76	4.24
A4	48.67	21.63	12.17	7.79	5.41	3.97
A5	46.31	20.58	11.58	7.41	5.14	3.78
A6	44.73	19.88	11.18	7.16	4.97	3.65
E	40.80	18.13	10.20	6.53	4.53	3.33
A7	40.92	18.19	10.23	6.55	4.55	3.34
A8	40.86	18.16	10.21	6.54	4.54	3.33
NA	40.85	18.15	10.21	6.54	4.54	3.33
KH	58.62	26.06	14.66	9.38	6.51	4.79

as

$$\alpha = \xi \frac{\Delta H}{RT} = \xi \frac{\Delta S}{R} \tag{21}$$

where ξ is a crystallographic factor depending upon the geometry of the molecules and has a value less than or equal to 1. $\Delta S/R$ (also known as Jackson's roughness parameter α) is the entropy of fusion (dimensionless) and R is the gas constant. When α is less than 2, the solid–liquid interface is atomically rough and exhibits nonfaceted growth. The value of Jackson's roughness parameter (α) is given in Table 1. For the entire solid dispersions, the α value was found to be greater than 2, which indicates the faceted [31] growth proceeds in all the cases.

Conclusion

The solid–liquid equilibrium phase diagram of NA–KH system shows the formation of simple eutectic alloy. The activity and activity coefficient values are very useful in computing thermodynamic mixing and excess functions. Thermodynamic excess and mixing functions g^{E} and ΔG^{M} values for eutectic and noneutectics are being found positive, which suggest the stronger association between like molecules, and there is nonspontaneous mixing in all the binary drugs.

Acknowledgment

The authors would like to thank the Head of the Department of Chemistry, V. K. S. University, Ara, Bihar, India, for providing research facilities.

References

[1] Murrey, F. M., & Srinivasan, A. (1995). *Biochem. Biophys. Res. Commun.*, *210*, 954–959.
[2] Murrey, F. M. (2003). *Clin. Infect. Dis.*, *36*, 453–460.

[3] Niren, N. M. (2006). *Cutis*, *77*, 11–16.
[4] Girgis, A. S., Hosni, H. M., & Barsoum, F. F. (2006). *Bioorg. Med. Chem.*, *14*(13), 4466–4476.
[5] Charles, P. H., & Estaleta, D. (1951). *Chem. Rev.*, *48*(3), 543–579.
[6] Trabalzini, L., Martelli, P., Bovalini, L., Dall'Acqua, F., & Sage, E. (1990). *J. Photochem. Photobiol. B: Bid.*, *7*, 317–336.
[7] Klaus, F. (1980). *Analytical Profiles of Drug Substances*, Vol. 9, Academic Press Inc.: London.
[8] de Leeuw, J., Assen, Y. J., van der Beek, N., Bjerring, P., & Martino Neumann, H. A. (2010). *J. Eur. Acad. Dermatol. Venereol.*, *10*, 1468.
[9] Del, S. R., Lazzoi, M. R., & Vasapollo, G. (2010). *Drug Deliv.*, *17*(3), 130–137.
[10] Bryn, S. R., Xu, W., & Newman, A. W. (2001). *Adv. Drug Del. Rev.*, *48*, 115–136.
[11] Remenar, J. F., Morissette, S. L., Peterson, M. L., Moulton, B., MacPhee, J. M., Guzman, H. R., & Almarsson, O. (2003). *J. Am. Chem. Soc.*, *125*, 8456–8457.
[12] Good, D. J., & Guez-Hornedo, N. R. (2009). *Cryst. Growth Dev.*, *9*, 2252–64.
[13] Shiraki, K., Takata, N., Takano, R., Hayashi, Y., and Terrada, K. (2008). *Pharm. Res.*, *25*, 2581–92.
[14] Ansari, M. T., Pervez, H., Shehzad, M. T., Mahmood, Z., Razi, M. T., Ranjha, N. M., & Khanum, N. (2012). *Pak. J. Pharm. Sci.*, *25*(2), 447–456.
[15] Aggarwal, A. K., & Jain, S. (2011). *Chem. Pharm. Bull.*, *59*(5), 629–638.
[16] Sangster, J. (1999). *J. Phy. Chem. Ref. Data*, *28*, 889–930.
[17] Sharma, B. L., Tandon, S., & Gupta, S. (2009). *Cryst. Res. Technol.*, *44*, 258–268.
[18] Malaviolle, R., De Maury, G., Chauvet, A., Terol, A., & Masse, J. (1988). *Thermochemi. Acta*, *121*, 283.
[19] Shekhar, H., & Salim, S. S. (2011). *J. Nat. Acad. Sci. Letter*, *34*, 117–125.
[20] Nieto, R., Gonozalez, M. C., & Herrero, F. (1999). *Am. J. Phys.*, *67*, 1096–1099.
[21] Agrwal, T., Gupta, P., Das, S. S., Gupta, A., & Singh, N. B. (2010). *J. Chem. Engg. Data*, *55*, 4206–4210.
[22] Shamsuddin, M., Singh, S. B., & Nasar, A. (1998). *Thermochemica. Acta*, *316*, 11–19.
[23] Singh, N. B., & Glicksman, M. E. (1989). *J. Cryst. Growth*, *98*, 573–580.
[24] Turnbull, D. (1950). *J. Chem. Phys.*, *18*, 768.
[25] Gunduz, M., & Hunt, J. D. (1989). *Acta Metall.*, *37*, 1839.
[26] Akbulut, S., Ocak, Y., Keslioglu, K., & Marasli, N. (2009). *Appl. Surf. Sci.*, *255*, 3594–3599.
[27] Hunt, J. D., & Lu, S. Z. (1994). In: D. T. J. Hurle (Ed.), *Handbook of Crystal Growth*, Elsevier: Amsterdam, p. 112.
[28] Chadwick, G. A. (1972). *Metallography of Phase Transformation*, Butterworths: London, p. 61.
[29] Wilcox, W. R. (1974). *J. Cryst. Growth*, *26*, 153–154.
[30] Hunt, J. D., & Jackson, K. A. (1966). *Trans. Metall. Soc. AIME*, *236*, 843.
[31] Shekhar, H., & Kant, V. (2011). *I. J. Chem. Soc.*, *88*, 947–952.